[1]Shivaji Raskar

[2]Sanjay Dambhare

Advancing Distance Relaying Reliability: S Transform Solution for Renewable Energy-Infused Smart Grid

Journal of Electrical Systems

Abstract: - Distance relaying is a crucial component in safeguarding transmission lines globally. However, the presence of Sub-Synchronous Resonance (SSR) introduces challenges, as oscillations in voltage and current magnitudes adversely affect the performance of conventional distance relays. Detecting faults accurately during these oscillations poses a significant challenge for traditional relaying mechanisms. This paper addresses the issue of SSR-induced maloperations in distance relays, particularly in the context of the increasing penetration of renewable energy resources in smart grids. The integration of wind power into the grid generates sub-synchronous oscillations, leading to protection issues. In response, a novel solution leveraging the S transform, a modern signal processing technique, is proposed to enhance the robustness of distance relaying under such challenging conditions. The developed algorithm is implemented in MATLAB and rigorously tested on the First Benchmark Model of sub-synchronous resonance. Simulation of the model is conducted in the PSCAD simulation software, and the results are thoroughly validated in MATLAB. The study demonstrates the efficacy of the S transform-based approach in accurately identifying faults and mitigating maloperations caused by SSR, thereby improving the reliability of distance relaying in smart grids with high renewable energy integration.

Keywords: Sub-synchronous resonance, S-transform, series compensation.

I. INTRODUCTION

The surge in electricity demand, the expansion of alternative energy sources, and the dynamic energy market have given rise to novel challenges in power grids. In the pursuit of augmenting transmission line capacity with minimal losses, electrical utilities have deployed advanced innovations and compensatory methodologies. Series compensation emerges as a cost-effective means to augment the load-handling capabilities of transmission lines, albeit with the drawback of introducing complications like sub-synchronous resonance (SSR) within the power system. Traditional relays exhibit malfunctioning tendencies when confronted with voltage and current magnitude oscillations associated with SSR, necessitating the implementation of an adaptive protection strategy to ensure the secure operation of relays.

Interactions between the mechanical torques of the turbine and the electrical power system results in power oscillations; this phenomenon on the power system is commonly referred to as sub-synchronous resonance. Data-based field analyses of sub-synchronous and super-synchronous oscillations are presented, along with applications for numerical relays, in [1].

This research demonstrates the time, frequency, and interdependence relationships between oscillating voltages and currents. Rotational torque interaction, control interaction, and SSR are the three categories under which sub-synchronous oscillations come in to picture. Using practical examples of sub-synchronous resonance analytics, damping and SSR prevention are easily achieved in [2]. The task force of the dynamic performance working group developed the first benchmark model of sub-synchronous resonance and directions for computer simulations in 1977 using actual values and implementation framework from the Navajo project. The operation of the Out of Step (OOS) protection function is controlled by an adaptive algorithm based on a subharmonic and time-domain analysis of ferro-resonance in accordance with the protection approach. Such failures happen during SSR on distance relays with Out of out-of-step blocking (OSB) elements. Thus, it is essential to choose an adaptive algorithm for distance relays.

A new algorithm estimates the sub-synchronous voltage across Thyristor-Controlled Series Capacitors (TCSC) due to sub-synchronous currents is proposed in [3]. In addition, theoretical analysis and frequency- based mitigation techniques are discussed in the paper. Through rigorous digital demonstrating, the paper [4] presents an accurate

[1] *Shivaji Raskar: College of Engineering, Pune

[2] Sanjay Dambhare, College of Engineering, Pune

eigen-analysis of Thyristor-Controlled Series Compensator (TCSC) compensated lines. The research in [5] examines sub-synchronous resonance in power systems with series compensated transmission lines using the modal repulsion phenomenon. This analytical method is extended to assess sub-synchronous resonance behavior in doubly-fed induction generators (DFIG). The research study [6] investigates the performance of DFIG in this setting by modelling sub-synchronous resonance without series compensation using a modified IEEE first test benchmark model. The present article explores using a scalable and mobile Gaussian window for localization as the basis for the S transform. The fundamental concepts of the Continuous Wavelet Transform (CWT) are expanded upon by the S transform, which is examined here. Interestingly, the S transform provides time-frequency-dependent resolution and maintains the exact correlation with the Fourier spectrum used in this work for fault detection and Sub-synchronous Resonance (SSR) [8].

A distance relay that uses power swing blocking techniques is developed in reference [9]. This research presents an approach that uses active and reactive power signals to detect symmetrical three-phase faults during power fluctuations. It is difficult to identify power swings from symmetrical flaws since they are symmetrical. To tackle this, reference [10] describes an innovative technique that uses a differential power- based method for symmetrical defect identification during power swings. Furthermore, [11] proposes a fault detection strategy during power swings that employ solely current signals through the amplitude modulation method to prevent distance relay maloperations [12].

This study aims to provide fault detection for accurate distance relay operation. When sub-synchronous oscillations trigger power swings on transmission lines, distance relay malfunctions may occur. At the generator bus, the signals for voltage and current are obtained, and the S-transform algorithm is used for processing. The time-frequency signals obtained from the S-transform are put into action to trip the distance relays on the transmission lines accurately.

II. SUB-SYNCHRONOUS RESONANCE ON POWER SYSTEM

Sub-synchronous resonance (SSR) involves the interaction of electrical parameters, specifically voltage and current frequencies, with the natural frequency of the rotating shaft due to series compensation. Torsional interactions, self-excitation induced by the induction generator effect, and torque amplification are the principal factors contributing to sub-synchronous resonance. The induction generator effect leads to self- excitation, representing a purely electrical phenomenon.

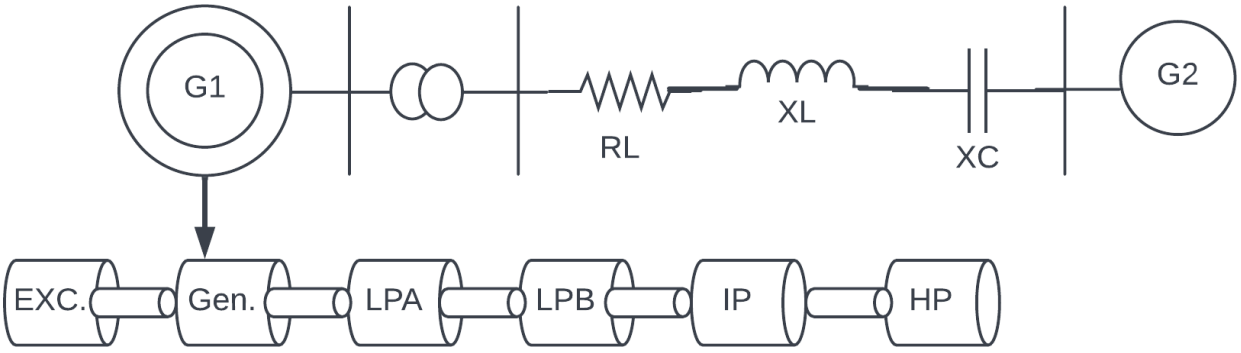

Figure 1: First benchmark model of SSR

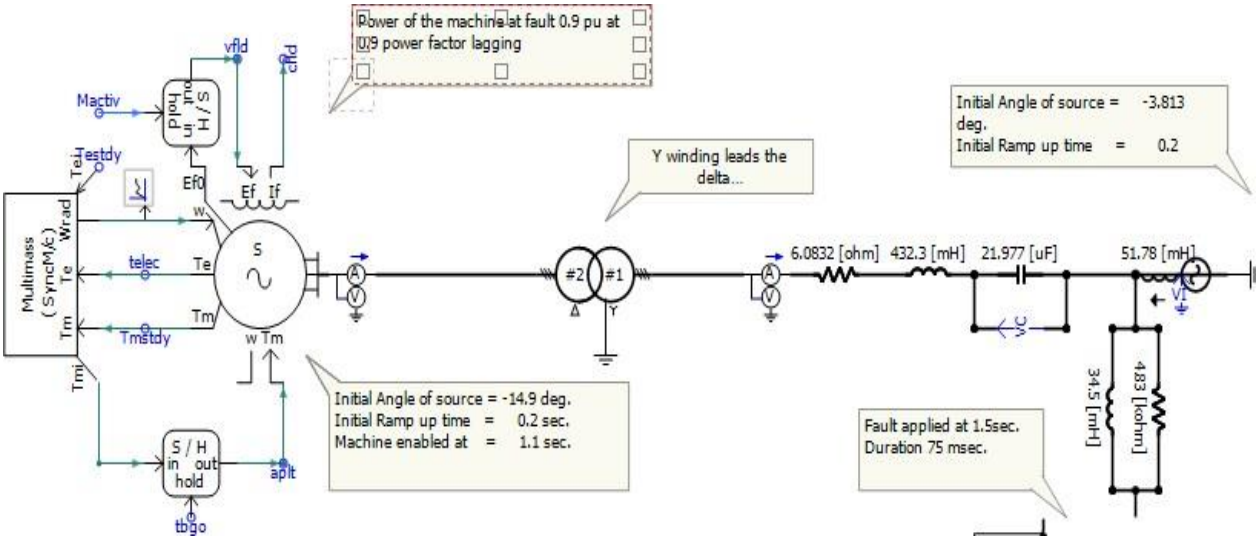

Figure 2: Representation of SSR model on PSCAD

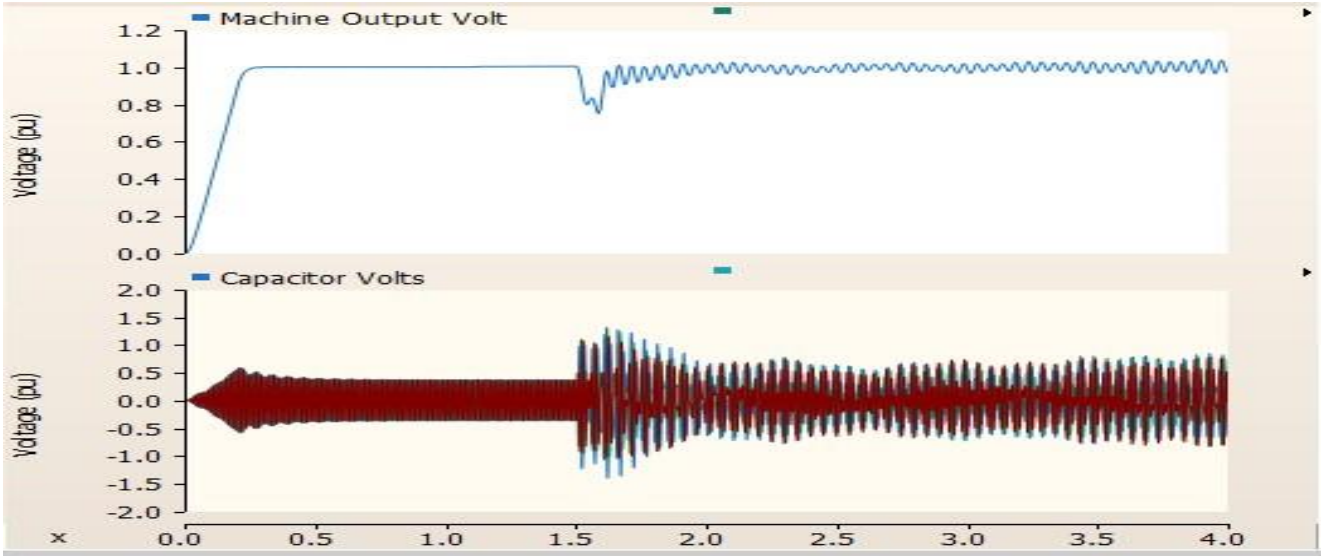

Figure 3: Voltage across compensating capacitor

In power systems, numerous transient events occur due to circuit breaker operations and the presence of faults on transmission lines. Series capacitors are employed to enhance system performance during power supply interruptions by minimizing the rotor angle difference of synchronous generators. Considering reactive power losses, transmission lines exhibit improved voltage regulation. Series-compensated trans- mission facilitates balanced power flow by adjusting the impedances of neighboring transmission grids and managing damping oscillations.

A Theoretical phenomenon of SSR

Below is a brief explanation of how SSR functions conceptually in an AC transmission network. The lodability of the transmission line is denoted by

$$P = \frac{V_i.V_j}{X_{Tij}}.sin\delta \qquad (1)$$

Where V_i and V_j are the voltage and current of the transmission line connecting the bus i and bus j. The inclusion of series capacitors, which lower the overall line impedance, enhances the power transfer capacity of series compensation and is represented by:

$$X_{Tij} = X_{Lij} - X_{Cij} \qquad (2)$$

$$X_{Tij} = (1 - S).X_{Lij} \qquad (3)$$

The amount of compensation may possibly reach 100%. If there are any little faults or abnormalities, this might generate large currents. On the other hand, excessive compensation exposes issues with protection relays and voltage profiles in case of a malfunction. In a power grid with radial series compensation, the electrical resonance frequency is expressed in the following form:

$$f_{er} = \pm f_s \sqrt{\frac{X_{Cij}}{X_{Lij}}} \tag{4}$$

Here, X_L represents the transmission line's inductive reactance, and f_s is the grid's system frequency. The current entering the grid interacts with the turbine-generator rotor at subharmonic frequencies within the generator's armature winding. The current includes the grid frequency as well as other sinusoidal components that are determined by the components of the utility that are currently in place, as shown in equation (5).

$$i(t) = K.[C.sin(\omega_1 t + \psi_1) + D.e^{-\xi\omega_2 t} sin(\omega_2 t + \psi_2) \tag{5}$$

the damping ratio represented by $\xi\omega$ is

$$\xi = \frac{R}{2}\sqrt{\frac{C_{ij}}{L_{ij}}} \tag{6}$$

The damping frequency is ω_2 as shown below:

$$\omega_2 = \omega_n\sqrt{1-\xi^2} \tag{7}$$

ω_n is the natural frequency in its undamped state, as shown below:

$$\omega_n = \sqrt{\frac{1}{L_{ij}C_{ij}}} \tag{8}$$

The sub-synchronous current induced in the generator generates the turbine-generator shaft torque. A sub-synchronous torque may meet one of the rotary system's natural frequencies. As a consequence, the shaft begins to oscillate at some natural frequencies. The turbine-generator shaft may experience catastrophic damage as a result of sub-synchronous resonance. SSR is typically separated into transient and steady states, as mentioned below:

Sub-synchronous frequencies are a subset of transient magnitudes and, therefore are depend on network characteristics. The generator's slip frequency, f_r, can be calculated using

$$fr = f0 - fer \tag{9}$$

The torque amplitude is considerably enhanced more substantially for the system without compensation if this frequency meets one of the natural frequencies of both the turbine-generator rotor (f_n). As shown in Fig. 3, voltage across the capacitor, which is placed on the transmission grid, is unstable after the SSR event. Also, torques on the multi-mass system of the generator start to increase, and natural fluctuations are shown in Fig. 4.

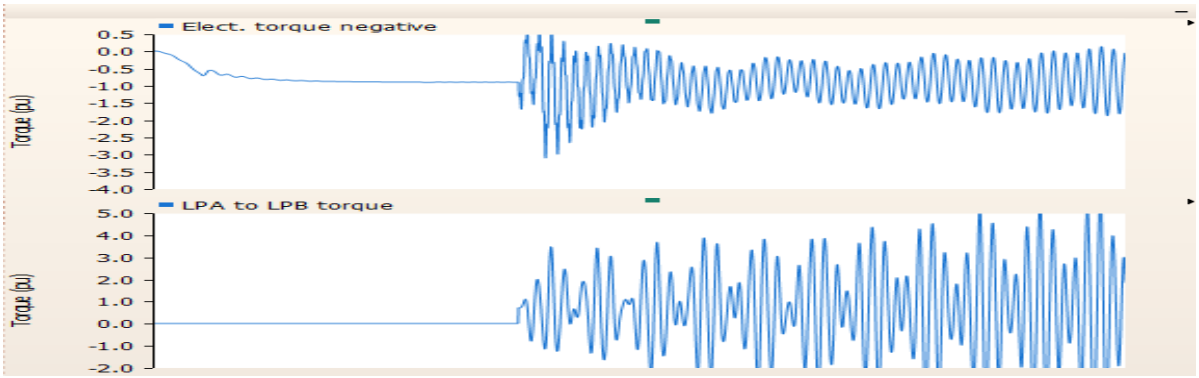

Figure 4: Electrical and Mechanical torques during SSR

Induction generator effect (IGE) and torsional interaction are two subtypes of steady-state (self- excitation) SSR. The generator is represented by IGE as a rigid mass linked to the network at a constant speed. Torsional interaction incorporates the multi-mass turbine generator, which interacts with fault condition at its natural frequencies.

III. PRINCIPAL OF FAULT DETECTION DURING SSR

A transient event, or system fault, causes a significant increase in the flow of current across the system. Numerous factors, including fault location, fault nature, fault time, fault resistance, and the network's pre-fault state, have significant effects on the current flow's magnitude. In contrast to what is seen during a power swing, the energy content of the current signal increases significantly, complying with a fault occurrence. Additionally, DC offset and symmetrical components in the current signal facilitate identifying and detecting challenges.

One modern mathematical method used in signal processing to determine the energy content of the current signal is the S transform. The paper presents a novel and trustworthy method for fault identification and detection during power fluctuations by utilizing the electrical current signal's energy content, and symmetrical components.

The Fourier transform has a few drawbacks, especially that it can only generate time-averaged spectra relevant to stationary time series [13]. Therefore, when dealing with time-series spectrum fluctuations, Fourier's time-averaged amplitudes must be increased, and more complex time-frequency representations must be used. The S transform is a technique that makes time-frequency analysis faster.

A. S transform

Local spectral phase features provide the time-frequency representation called the S transform. It strongly correlates with Fourier analysis and provides a wavelet-like relative bandwidth analysis. Wavelet and Short Time Fourier Transform (STFT) components are incorporated into this invertible time-frequency spectral identification method [14]. A frequency-invariant amplitude response is obtained. Precise alignment of local spectrum analysis with a frequency-dependent resolution in the time-frequency space is an important aspect of the S transform. It can be conceived as a step-corrected wavelet-based transform.

The S transform provides a frequency-dependent resolution by using an analysis window whose width decreases with frequency. This maintains each frequency's absolute phase information and enables multi-resolution analysis. The following is the expression for a function $x(t)$'s continuous S transform:

$$S(\tau, f_n) = \int x(t) \frac{|f_n|}{\sqrt{2\Pi}} e^{\frac{-(\tau-t^2)f_n^2}{2}} e^{-i2\Pi f_n t}\, dt \tag{10}$$

A voice S(τ, f_0) is characterized as a one-dimensional function of time for a fixed frequency f_0. This function delineates the variations in amplitude and phase corresponding to the specified frequency as they evolve over time.

$$S(\tau, f_0) = A(\tau, f_0)\, e^{i\phi(\tau, f_0)} \tag{11}$$

A local spectrum, denoted as S(τ_0, f), is a one-dimensional function of frequency for a fixed time t_0. The S

transform serves as a representation of the local spectrum, and the averaging of these local spectra over time results in the Fourier spectrum.

$$H(f) = \int S(\tau, f)\, d\tau \tag{12}$$

Here, $H(f)$ represents the Fourier transform of $h(t)$. In a discrete formulation, the S transform of a discrete time series $h[kT]$ is expressed as:

$$S[j\tau, \frac{n}{NT}] = \sum H\,[\frac{m+n}{NT}]\, e^{\frac{-2\Pi^2 m^2}{n^2}} \tag{13}$$

Here, the indices j, m, and n vary within the range of 0 to $N-1$. The energy, denoted as E, of the signal is derived from the S transform as referenced in [12].

$$E = abs(S(j,n))^2 \tag{14}$$

For analytical purposes, we will exclusively consider the fundamental voice of the S transform.

$$E = abs(S(j, n_{fund}))^2 \tag{15}$$

A. Sequence Components

Charles L. Fortescue introduced the method of sequence components in [8]. This method is employed for analyzing power systems operating under fault conditions. In a 3ϕ unbalanced system, there are six degrees of freedom, whereas a 3ϕ balanced system has only two degrees of freedom.

Consequently, a 3ϕ unbalanced system can be decomposed into three sets of the balanced system, each possessing two degrees of freedom. In a 3ϕ system with the phase sequence a-b-c, these three sets of balanced phasors are identified as positive (subscript 1), negative (subscript 2), and zero (subscript 0).

$$\begin{bmatrix} I_{a0} \\ I_{a1} \\ I_{a2} \end{bmatrix} = \frac{1}{3}\begin{bmatrix} 1 & 1 & 1 \\ 1 & \alpha & \alpha^2 \\ 1 & \alpha^2 & \alpha \end{bmatrix} \begin{bmatrix} I_a \\ I_b \\ I_c \end{bmatrix} \tag{16}$$

where $\alpha = e^{j2\Pi/3}$.
Sequence components are nonexistent during power swings but manifest during asymmetrical faults. In instances of symmetrical faults, both negative and zero sequence components are absent. An algorithm has been devised to address this specific scenario.

B. Computation of Energy

Utilizing current samples acquired at both ends, the energy content in the current signals, denoted as E_1 and E_2, is determined through the application of equation (14). Subsequently, the absolute value of the difference in the energies is computed.

$$\Delta E = \text{abs}(E1 - E2) \tag{17}$$

The difference is computed to take into account energy changes that may occur during a power swing brought on by SSR.

IV. Fault Detection Criteria

The occurrence of a fault on a phase is identified when the value of ΔE surpasses the predefined threshold (E_{set} = $1*10^7$), coupled with the presence of a dc offset in that phase. In instances where the dc offset is absent but ΔE exceeds the threshold, the existence of symmetrical components is examined. If symmetrical components are detected, the fault is identified on that phase.

For a single line to ground fault, the condition for ΔE is evaluated on the relevant phase, and the presence of a dc offset on that phase dictates the trip decision. In the absence of a dc offset, the trip decision is contingent on the presence of a zero sequence component.

V. CASE STUDIES AND RESULTS

Before The proposed algorithm is tested on the First Benchmark Model of sub-synchronous resonance. The system is modeled in PSCAD environment, and the algorithm is coded in MATLAB.

A. Behavior of distance relay in the presence of SSR without any permanent fault

Subsynchronous resonance occurred, and power swings started to rise due to a small disruption on the transmission line at 0.0166 seconds. Voltage and current measurements were taken close to the generator bus are oscillatory in nature due to the power swings, depicted in Fig. 5. Torques of the various stages for the multimachine system are observed on and verified for the sub-synchronous resonance condition. The line is series compensated 75 % with respect to the inductance of the transmission line. Distance relay placed at the generator bus is operated on the signals given by voltage and current measurements, starting to be maloperated in the presence of such a situation. Fig. 6 shows the distance relay behavior in the presence of the sub-synchronous oscillations without any fault, and Fig. 7 shows the faulty relay tripped in zone 1 without any permanent fault. To estimate the adaptive first zone settings for distance relay, the V_{ref} or control value of the SSSC, is set within ±0.1 p.u. The SSSC enters the system at 1.05 seconds after connecting at the halfway point. When SSSC consumes inductive reactive power, the midpoint voltage drops relative to the standard working voltage when SSSC is absent. As a result, the relaying bus voltage decreases and the distance relay's perceived impedance is also reduced, leading to over-reach. Fig. 6 illustrates the simulation result of an adaptive distance relay for power flow in forward from P to Q is adaptively decreased when SSSC is linked to the system at 1.05 seconds and absorbs the reactive power of the inductive, settling to 0.7671 per unit of distance value after 13 milliseconds to achieve a new first zone adaptive setting.

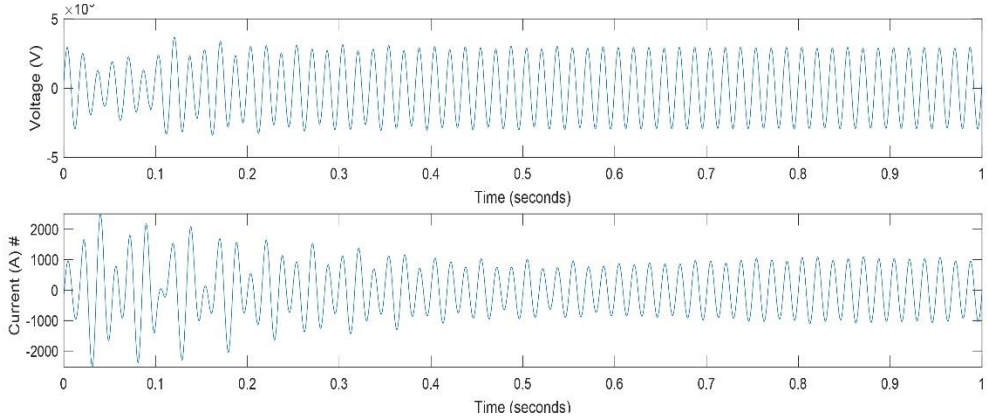

Figure 5: Voltage and current during No fault condition

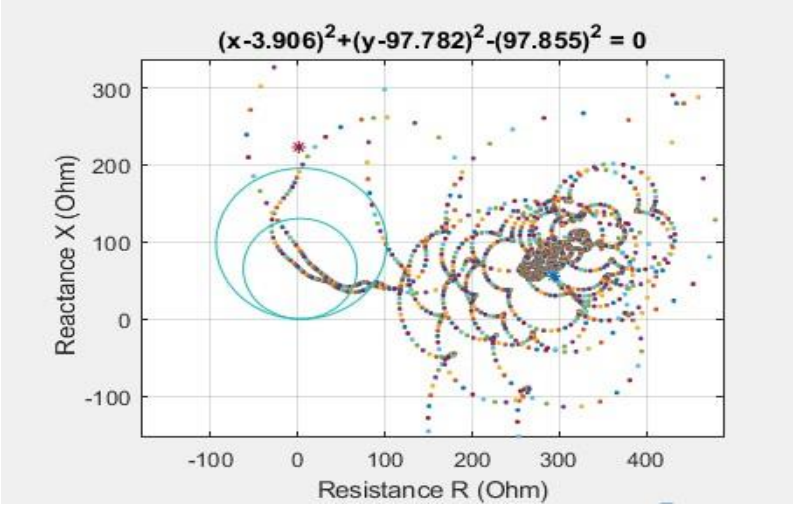

Figure 6: Relay characteristics during No fault condition

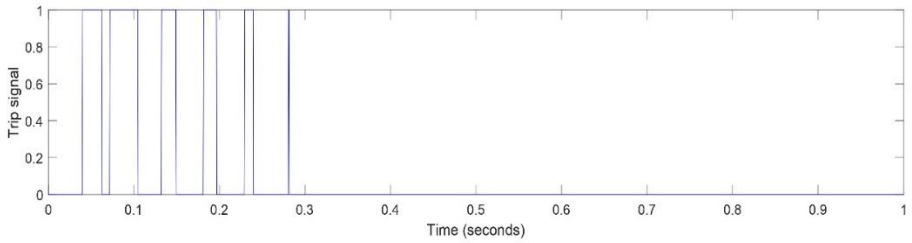

Figure 7: Trip signal of the distance relay without any fault

B. Behavior of Distance Relay in the Presence of SSR with Fault

Distance relay starts to maloperate without any fault on the transmission line. To avoid such maloperation, an S-transform based fault detection scheme is simulated and verified here. Fig. 8 shows voltage and current waveform in the presence of the sub-synchronous oscillations, and the fault occurs on the transmission line at o.8 seconds.

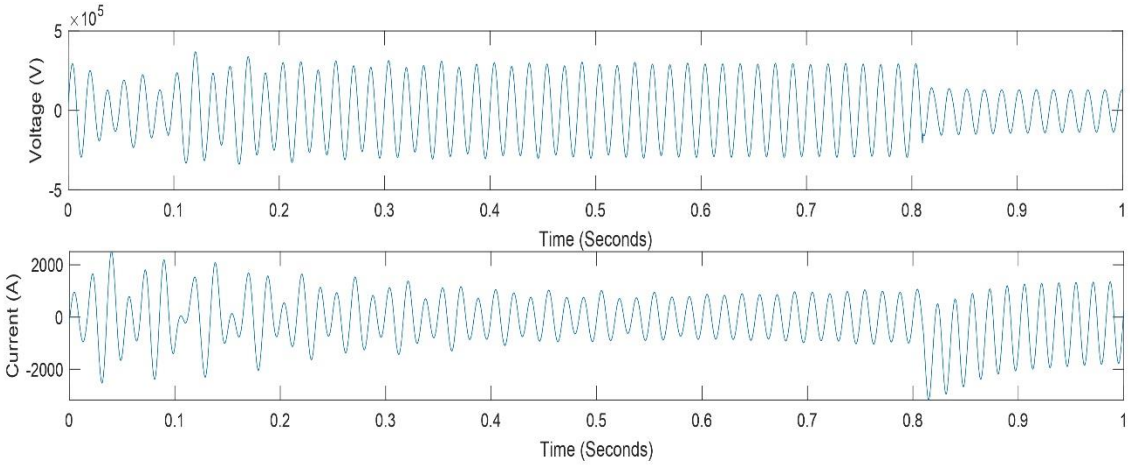

Figure 8: Voltage and current waveform for symmetrical fault 50 km from bus 1 at 0.8 seconds in the presence of sub-synchronous oscillations.

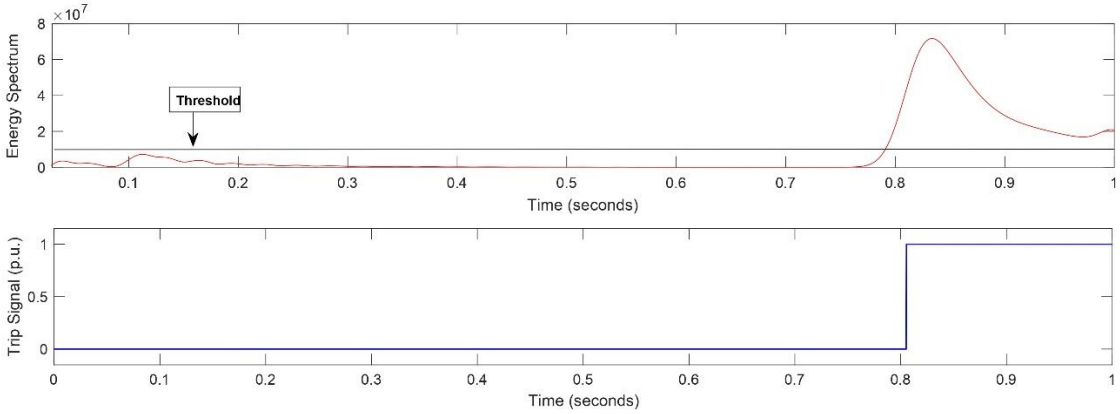

Figure 9: Correct trip for symmetrical fault 50 km from bus 1 at 0.8 seconds in the presence of sub-synchronous oscillations.

The Energy function E is computed by using voltage and current signals, and its characteristics are shown in Fig. 9. When the energy function characteristics cross its threshold value trip decision is given to the distance relay, at

0.8 seconds the relay is tripped for the fault on the transmission line at the 50 km length at the time of 0.8 seconds. Fig. 11 shows the adaptive mho relay reach, depicted in black, and the conventional relay reach, displayed in red. Relay reach is observed to increase adaptively with SSSC setting value Vref = 0.1 p.u. when compared with conventional relay reach. In a similar vein, the distance relay setting factor becomes adaptable when SSSC injects reactive power, both capacitive and inductive. For Vref = - 0.1 p.u., the adaptive setting factor takes around 1.5 cycles to settle, while it takes about 3 cycles to settle for Vref = 0.1 p.u. The reason for this is the usage type PI controller and has its own settling time constant, which is shown in the report's modeling of the SSSC.

The relay lookup table includes the adaptive relay settings computed and stored for varying compensation modes and levels. In order to identify and pinpoint the fault location that causes the relay to become adaptive, the pre-calculated setting is employed by the adaptive relay in response to feedback from the compensation (Vijn). These lookup table settings are for the 20 planned systems; the settings can be determined to load into the relay lookup module for any other system by utilizing the adaptive relay equation and other pertinent variables. The adaptive relay alternative to the associated issue of traditional distance relay's underreach and overreach. It is essential to look for boundary conditions, including when a fault occurs in front of the first zone setting for overreach settings in various compensation modes or near to the first zone of protection for underreach settings.

C. Sub-Synchronous Oscillations With the Interfacing of Renewable Energy Sources to Grid

Renewable energy resources like solar panels and wind farms are included in the smart grid to supply local loads. A 400 MVA wind farm is modeled by a DFIG Fig. 10. A two-mass Wind turbine coupled with a generator is connected to the HV network by a 230/13.8 kV transformer. It rotates at variable wind speed to generate power at constant voltage and frequency by employing AC/DC converters connected to the rotor and stator. The impact of ferro-resonance on the effect of line and plant outage in the network is analyzed on electrical and mechanical parameters of DFIG. The network connects the wind farm to 230 kV sides of no-load transformers. As shown in Fig. 5, SSO causes increasing and misshaping voltage and current waveforms in the network (230 kV side) and also in the wind farm (13.8 kV side) plant outage. SSO of wind farms causes increasing and oscillating mechanical parameters of DFIG. The mechanical position of the turbine deviates with respect to the generator up to 0.5^0 . The mechanical speed of the turbine has decreasing manner. Oscillatory decreasing of the speed causes oscillation of power in the wind farm.

The algorithm is examined at different compensation levels to attain other modes of natural frequencies to certify the correct operation. To do so, the inductance value of the lines (XL) is remained constant, then by changing compensation level and consequently XC the value of fer is changed and causes variety of natural frequency modes.

Regarding implementation of the relay with adaptive algorithm in a real power system some special considerations must be taken as follows. As was discussed in advance, PSL requires results of electrical studies, to determine behavior of the relay in SSR and ferro-resonance condition introduces universal protection software, which performs real-time electrical studies in the network to design protective system based on protection design criteria applicable to both traditional network and smart grid. This software is also able to consider impact of fault ride-through on wind turbine examined in various fault and ab- normal scenarios in the system. Hence, a practical power system requires incorporation of such analysis software with variety of adaptive algorithms designated to protective relays. Another concern respecting implementation of the relay in a real power system is capability of the algorithm in speed of the analysis and data reporting rate. Generally, speed of the data communication between above-mentioned analysis software and the relay and also modification of setting quantities must be high enough to address critical clearing time (CCT), which is calculated by the analysis software. In other word, the protective relay must be in new setting quantities before CCT becomes elapsed to maintain stability of the system in abnormal conditions.

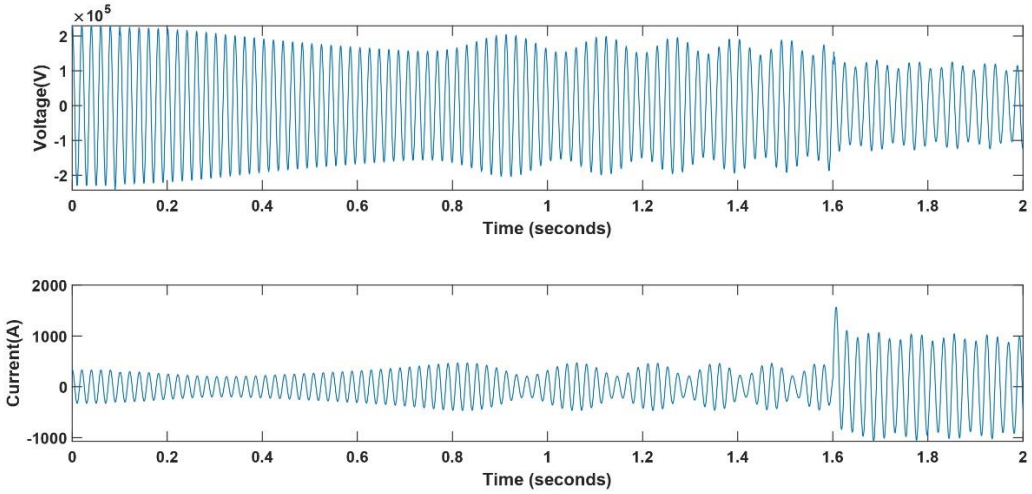

Figure 10: Voltage and current during SSO due to renewable integration with fault on the line at 1.6 seconds

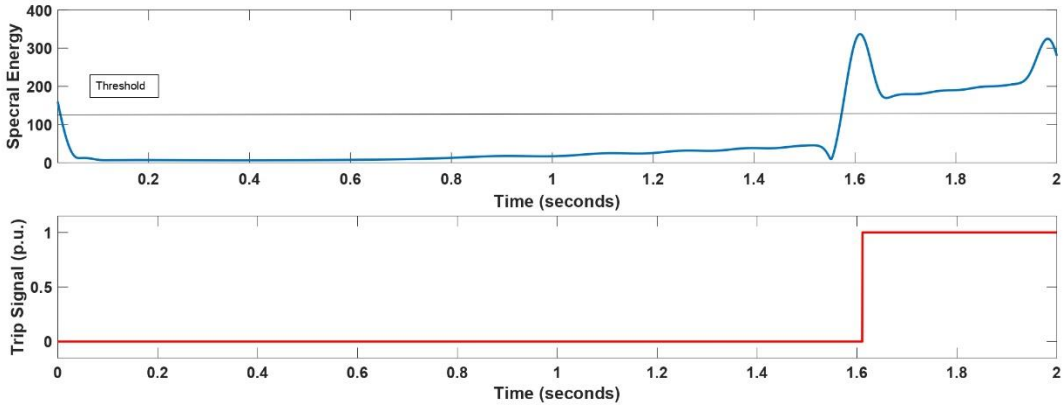

Figure 11: Trip During SSO

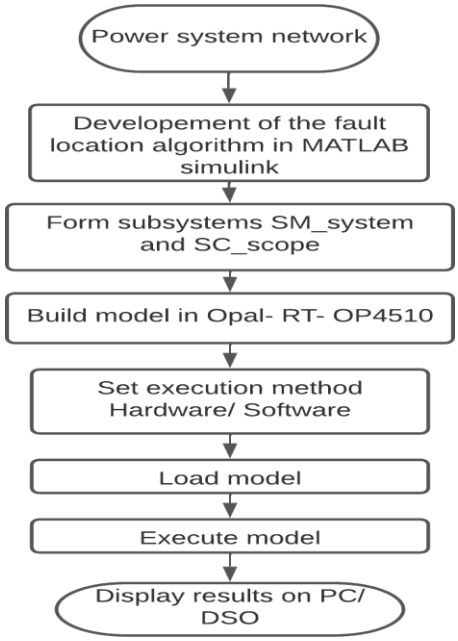

Figure 12: Flowchart for the execution of the algorithm on OPAL-RT-OP451

D. SSR analysis on OpalRT-OP4510

To verify the performance of the proposed algorithm in real-time simulators, it is required to modify the power system model into its twin model compatible with real-time simulators for the virtual-virtual representations. Real-time simulator Opal-RT-OP4510 is a high computing tool for the improved real-time performance of the algorithms. IEEE-39 bus New England test system is designed into MATLAB/Simulink, an advanced software tool compatible with Real-Time Workshop (RTW) and Real-Time Windows Target (RTWT) [15]. The IEEE 39-bus New England system with fault location algorithm is combined with one subsystem SM_{system}, and scope with OPPCOM block is another subsystem SC_{scope} with inter-connection to each other. The waveforms of voltage, current, and power (active and reactive), multimass torque systems are verified before implementing the fault location algorithm on the host computer and digital oscilloscope. Fig.12 shows the procedure for the execution of the algorithm. The subsystems with power-GUI block for Opal-RT-OP4510 are shown in Fig. 13. Actual output of real-time simulator Opal-RT-OP4510 with the host computer with virtual output are shown in Fig. 14.

Figure 13: Simulation set up for SM-System and SM-Scope

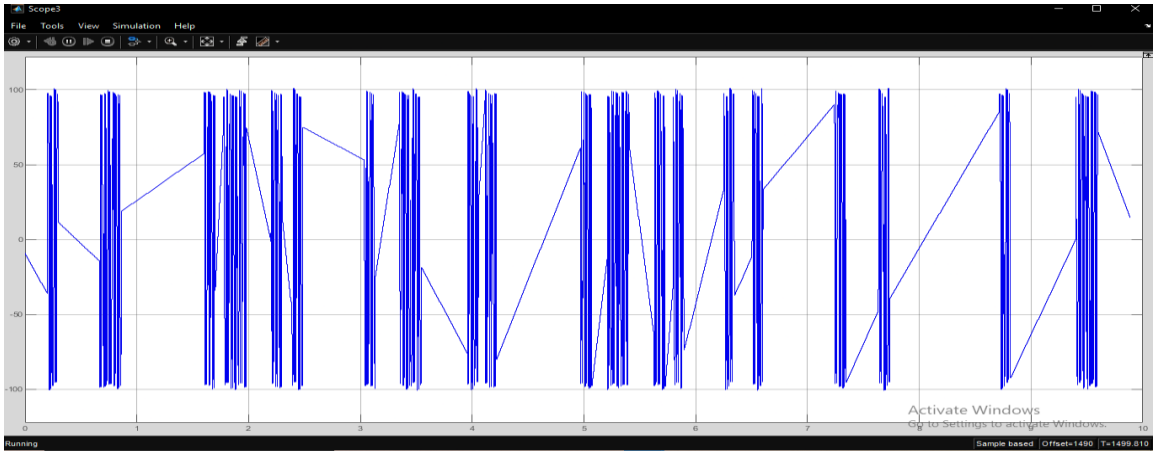

Figure 14: Simulation In Loop result on host computer system

VI. CONCLUSION

Here, a new S-transform-based fault detection-based backup protection scheme is proposed in this paper. Voltage and current measurements are collected at the generator bus and used to compute S-transform. Using S-transform SSR on the power grid is detected and provides correct tripping action to the distance relay in the presence of the sub-synchronous oscillations. The algorithm is tested for the various faults on the First Benchmark model of the Sub-Synchronous resonance. The test model is designed in the PSCAD.

ACKNOWLEDGMENT

We thank the Center of Excellence in Smart Renewable Energy Systems (CoE-SRES) and Technical Edu- cation Quality Improvement Programme-III (TEQIP-III) at the College of Engineering, affiliated to S. P. Pune University, Pune (India), for supporting the work.

REFERENCES

[1] T. Bengtsson, S. Roxenborg, M. M. Saha, P.O. Lindstrm, H. Eriksson, and M. Lindstrm, “Case studies and experiences with sub-synchronous resonance (SSR) detection technique," in 2016 Power Systems Computation Conference (PSCC), pp. 1-6, 2016.

[2] R. N. Damas, Y. Son, M. Yoon, S.-Y. Kim, and S. Choi, “Subsynchronous oscillation and advanced analysis: A review," IEEE Access, vol. 8, pp. 224020- 224032, 2020.

[3] B. Gao, H. Liu, H. Su, Z. Hong, C. Ji and M. Zhao, “Design and typical application of digital twin architecture in Smart Grid," 2022 7th Asia Conference on Power and Electrical Engineering (ACPEE),Hangzhou, China, April 2022.

[4] T. K. Oh and Z. Z. Mao, “Analysis on thyristor controlled series capacitor for subsynchronous resonance mitigation," IEEE International Symposium on Industrial Electronics Proceedings, vol. 2, pp. 1319-1323 vol.2, 2001

[5] S. R. Joshi and A. M. Kulkarni, “Analysis of SSR performance of TCSC control schemes using a modular high bandwidth discrete-time dynamic model," IEEE Transactions on Power Systems, vol. 24, no. 2, pp. 840- 848, 2009.

[6] W. Du, C. Chen, and H. Wang, “Subsynchronous interactions induced by dfigs in power systems without series compensated lines," IEEE Transactions on Sustainable Energy, vol. 9, no. 3, pp. 1275- 1284, 2018.

[7] S. Rezaei, "Behavior of Protective Relays During Subsynchronous Resonance in Transmission Line and Adaptation of Generator Out-of-Step Protection," in IEEE Transactions on Industry Applications,vol. 55, no. 6, pp. 5687-5698, Nov.-Dec. 2019

[8] R. Stockwell, L. Mansinha, and R. Lowe, “Localization of the complex spectrum: the s transform,"IEEE Transactions on Signal Processing, vol. 44, no. 4, pp. 998- 1001, April 1996.

[9] N. Z. Mohamad, A. Farid Abidin, and W. N. W. A. Munim, “A new tracking method of symmetrical fault during power swing based on s-transform," in 2012 IEEE International Power Engineering and Optimization Conference Melaka, Malaysia, pp. 141-146, 2012.

[10] A. Pradhan and G. Rao, “Differential power based symmetrical fault detection during power swing," in 2013 IEEE Power Energy Society General Meeting, pp. 1-6, 2013.

[11] P. N. Gawande and S. S. Dambhare, “A novel unblocking function for distance relay to detect symmet rical faults during power swing," in 2016 IEEE Power and Energy Society General Meeting (PESGM), pp. 1-6, 2016.

[12] S. Raskar, P. Gawande and S. Dambhare, "Wide-Area Measurement Assisted Algorithm for Secure Backup Protection during Stressed Conditions," 2021 9th IEEE International Conference on Power Systems (ICPS), Kharagpur, India, 2021, pp. 1-6

[13] “First benchmark model for computer simulation of subsynchronous resonance," IEEE Transactions on Power Apparatus and Systems, vol. 96, no. 5, pp. 1565-1572, 1977.

[14] R. G. Stockwell, L. Mansinha and R. P. Lowe, “Localization of the complex spectrum: the S trans- form," in IEEE Transactions on Signal Processing, vol. 44, no. 4, pp. 998-1001, April 1996

[15] S. K. Singh, B. P. Padhy, S. Chakrabarti, S. N. Singh, A. Kolwalkar and S. M. Kelapure, "Development of dynamic test cases in OPAL-RT real-time power system simulator," 2014 Eighteenth National Power Systems Conference (NPSC), Guwahati, India, 2014